Cell Research (2012) 22:1022-1033.

www.nature.com/cr

ORIGINAL ARTICLE

Microglial migration mediated by ATP-induced ATP release from lysosomes

Ying Dou[1, *], Hang-jun Wu[2, 3, *], Hui-quan Li[2], Song Qin[1], Yin-er Wang[2], Jing Li[2], Hui-fang Lou[2], Zhong Chen[2], Xiao-ming Li[2], Qing-ming Luo[3], Shumin Duan[2]

[1]Institute of Neuroscience and Key Laboratory of Neuroscience, Shanghai Institutes for Biological Sciences, Chinese Academy of Sciences, Shanghai 200031, China; [2]Department of Neurobiology, Key Laboratory of Medical Neurobiology of the Ministry of Health of China, Key Laboratory of Neurobiology of Zhejiang Province, Zhejiang University School of Medicine, Hangzhou, Zhejiang 310058, China; [3]Huazhong University of Science and Technology, Wuhan, Hubei 430030, China

Microglia are highly motile cells that act as the main form of active immune defense in the central nervous system. Attracted by factors released from damaged cells, microglia are recruited towards the damaged or infected site, where they are involved in degenerative and regenerative responses and phagocytotic clearance of cell debris. ATP release from damaged neural tissues has been suggested to mediate the rapid extension of microglial process towards the site of injury. However, the mechanisms of the long-range migration of microglia remain to be clarified. Here, we found that lysosomes in microglia contain abundant ATP and exhibit Ca^{2+}-dependent exocytosis in response to various stimuli. By establishing an efficient *in vitro* chemotaxis assay, we demonstrated that endogenously-released ATP from microglia triggered by local microinjection of ATPγS is critical for the long-range chemotaxis of microglia, a response that was significantly inhibited in microglia treated with an agent inducing lysosome osmodialysis or in cells derived from mice deficient in Rab 27a (ashen mice), a small GTPase required for the trafficking and exocytosis of secretory lysosomes. These results suggest that microglia respond to extracellular ATP by releasing ATP themselves through lysosomal exocytosis, thereby providing a positive feedback mechanism to generate a long-range extracellular signal for attracting distant microglia to migrate towards and accumulate at the site of injury.

***Keywords*:** microglia; migration; ATP; lysosome

Cell Research (2012) **22**:1022-1033. doi:10.1038/cr.2012.10; published online 10 January 2012

Introduction

Microglia are resident immune cells in the central nervous system (CNS). In response to injury or inflammatory stimuli, the resting microglia can be rapidly activated to participate in pathological responses, including migration to the affected site, release of various inflammatory molecules, and clearing of cellular debris [1, 2]. ATP released from damaged neural cells has been considered as the major chemokine for inducing rapid process extension and cell body migration of microglial cells [3-5]. However, ATP leaking from the local injured cells may not be able to diffuse extensively to effectively induce migration of remote microglia, because extracellular nucleotides are rapidly degraded by ecto-ATPases in the brain [6-8]. It seems likely that ATP released from injured neural tissue may evoke a regenerative ATP-induced ATP release from surrounding cells to establish the long-range extracellular ATP gradient required for the chemotaxis of remote microglia.

Lysosomes are traditionally considered as simply end organelles in cellular degradation pathways, but recent studies demonstrate their more essential roles in signal transduction pathways, through internalization of receptor-ligand complexes and secretion of signaling molecules [9-12]. Cells derived from the hemopoietic lineage use the lysosomal compartment as a regulated secretory organelle, defined as secretory lysosomes or lysosome-related organelles [9, 10]. Microglia are resi-

*These two authors contributed equally to this work.
Correspondence: Shumin Duan
Tel: 86-571-88208001
E-mail: duanshumin@zju.edu.cn
Received 6 March 2011; revised 28 September 2011; accepted 13 December 2011; published online 10 January 2012

dent CNS leukocytes and thus may also use lysosomes to secrete signaling molecules. Indeed, lysosomes in monocytes and microglia may be involved in cytokine release [13-15], although the detailed mechanisms have not been explored. Furthermore, lysosomes in astrocytes contain abundant ATP [16] and exhibit Ca^{2+}-dependent exocytosis in response to various stimuli [16-18]. In the present study, we asked whether microglia also release ATP through lysosome exocytosis and whether such a signaling pathway contributes to microglial chemotaxis. To address these questions, we established an *in vitro* chemotaxis assay using the micropipette ejection method, in a manner similar to that used for neuronal growth cone turning assay described previously [19]. We found that ATP-induced ATP release from microglial lysosomes contributed to the directional migration of remote microglia.

Results

Involvement of endogenously-released ATP in ATPγS-induced microglial chemotaxis

To efficiently and quantifiably analyze microglial chemotaxis, we established a reliable *in vitro* assay system using the focal micropipette ejection method, in which pulses of solution containing chemoattractant were repetitively pressure-ejected into microglial cultures at a defined frequency and pulse duration to create a microscopic gradient of the chemoattractant around the pipette tip (Figure 1A and Supplementary information, Movie S1). The concentration of the applied agent at 100 μm from the pipette tip was estimated to be 1 000-fold lower than that in the pipette [19]. In response to pulse application of ATP (1 mM in pipette), microglia showed rapid (within a few minutes) dynamic changes in cell morphology, including extension of processes, formation of a membrane ruffle at the leading edge of the cell, and migration of the cell body toward the pipette tip (Figure 1A and 1C, Supplementary information, Movie S1). Application of the non-hydrolyzable ATPγS induced similar chemotaxis of surrounding microglial cells in a dose-dependent manner (Figure 1B and 1C, Supplementary information, Movie S2).

The ATPγS-induced microglial chemotaxis was largely prevented in the presence of the P2Y receptor antagonist reactive blue 2 (RB-2, 2 μM) (Figure 2A and 2C, Supplementary information, Movie S3), consistent with the involvement of P2Y receptors reported previously [4, 20]. Interestingly, when the medium contained apyrase, which hydrolyzes ATP but not ATPγS [7], the ATPγS-induced migration of microglia, especially those remote (140-250 μm) from the pipette tip, was significantly inhibited

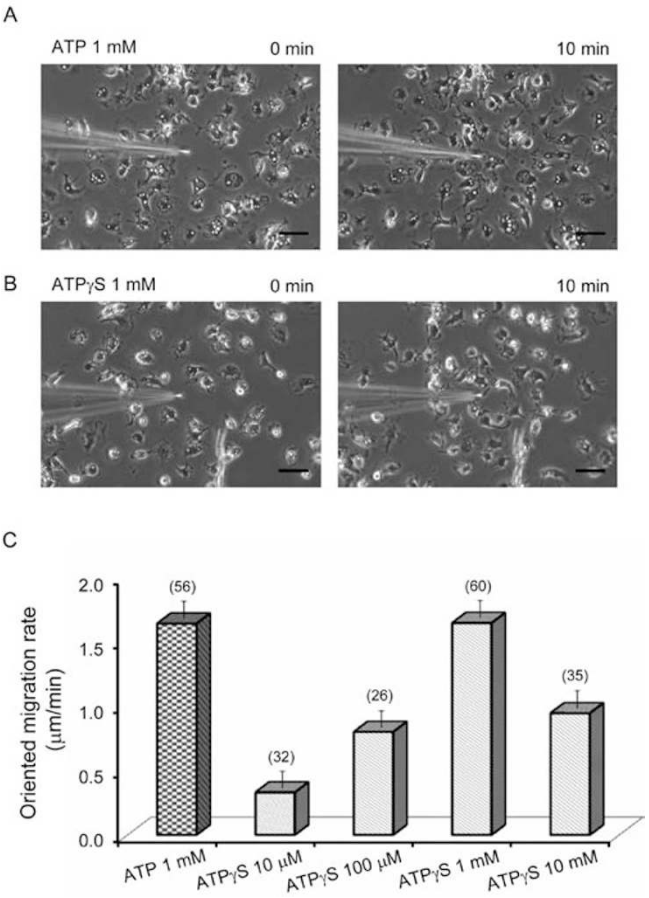

Figure 1 ATP induces oriented migration of microglia. **(A**, **B)** Example microscopic images showing cultured microglia migrating toward the pipette tip at the center of the field 10 min (right panels) after exposure to an ATP **(A)** or ATPγS **(B)** gradient created by pulsatile application (1 mM in the pipette). Images in **A** and **B** were taken from the same fields as those shown in Supplementary information, Movies S1 and S2, respectively. Scale bars, 50 μm. **(C)** Averaged oriented migration rates of microglia induced by a gradient of ATP (1 mM in the pipette) or ATPγS (various concentrations in the pipette as indicated). The number associated with each column refers to the number of cells examined.

(Figure 2B-2D, Supplementary information, Movie S4), suggesting that ATP released from microglia themselves played a critical role in the ATPγS-induced microglial migration. Consistent with this notion, we found that application of ATPγS through micropipette induced apparent elevation of extracellular ATP, as revealed by the increased NADH fluorescent signal produced by enzyme reaction when ATP is released (Supplementary information, Figure S1).

We found that apyrase and RB-2 not only inhibited ATPγS-induced cell morphology change and migration, but also reduced basal cell motility to 73.87% ± 0.03%

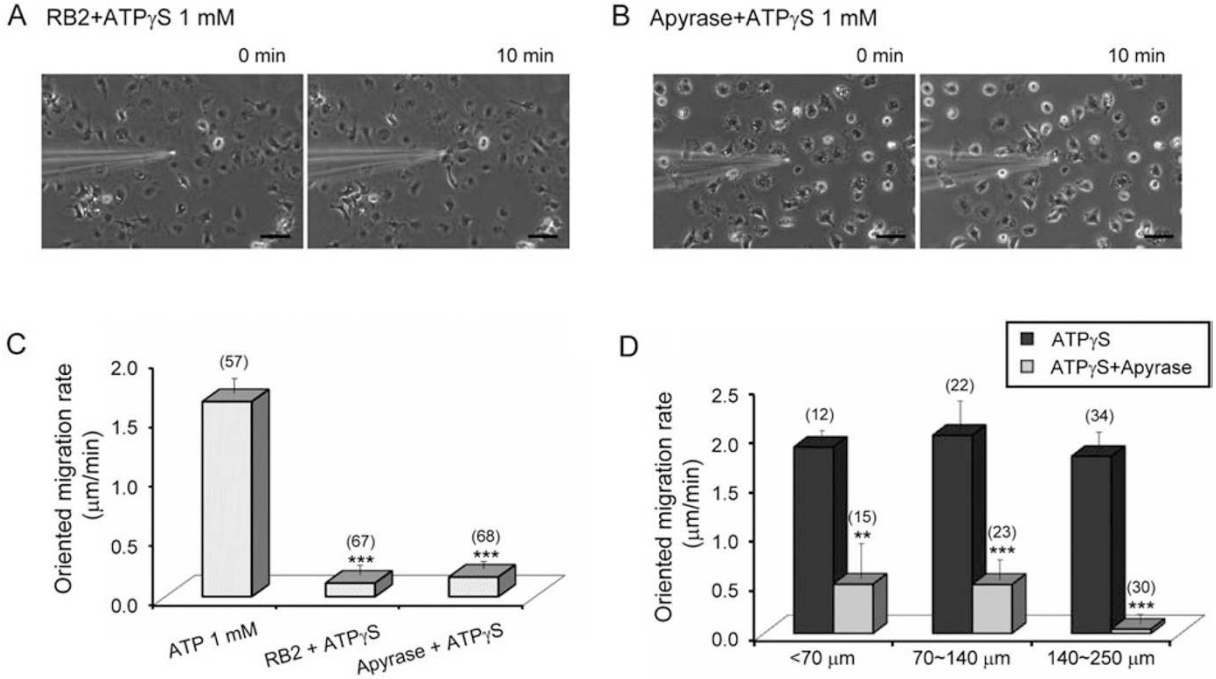

Figure 2 Involvement of P2Y receptors and endogenously-released ATP in ATPγS-induced microglial migration. **(A**, **B)** Example microscopic images of cultured microglia before (0 min) and 10 min after exposure to the gradient of ATPγS (1 mM in the pipette) in the presence of the P2Y receptor antagonist RB-2 (2 μM, **A**) or the ATP degradation enzyme apyrase (30 U/ml, **B**). Images in **A** and **B** were taken from the same fields as those shown in Supplementary information, Movies S3 and S4, respectively. Scale bars, 50 μm. **(C)** Averaged migration rates of microglia induced by ATPγS in conditions shown in **A** and **B**. **(D)** Differential inhibition by apyrase of the oriented migration of microglia located in three areas at different distances from the tip of the pipette puffing 1 mM ATPγS. Note greater inhibition by apyrase of the migration of remote microglia (located between 140 and 250 μm from the pipette tip). The number associated with each column in **C** and **D** refers to the number of cells examined. $^{**}P < 0.01$ and $^{***}P < 0.001$ compared with the corresponding control group (without inhibitors).

and 75.28% ± 0.02% of the control, respectively, consistent with the idea that endougeous ATP release from microglia also contributes to the spontaneous cell mobility.

Ca^{2+}-dependent lysosomal exocytosis in microglia

Lysosomes in astrocytes have been reported to secrete ATP in response to various stimuli [16]. To identify ATP-containing vesicles in microglia, we loaded the cultures with quinacrine, an ATP marker that is used to locate intracellular stores of ATP [21, 22]. We found that quinacrine accumulated in lysosomes labeled with LysoTracker Red DND-99 (Lysotracker, Figure 3A and 3D), with a fluorescence intensity apparently stronger than that accumulated in mitochondria labeled with MitoTracker Red CM-H_2XRos (Mitotracker, Figure 3C). Similarly, mant-ATP (2'-(or-3')-O-(*N*-methylanthraniloyl) adenosine 5' -triphosphate), a fluorescent nucleotide analogue used for studying ATP stores and nucleotide-binding proteins [16, 23], also selectively labeled lysosomes in microglia (Figure 3B and 3D). Furthermore, perfusion with glutamate or potassium cyanide (KCN), an inhibitor of oxidative phosphorylation that is used to induce chemical hypoxia [24], resulted in apparent mant-ATP release, as indicated by a significant decrease in the fluorescence intensity of the mant-ATP signal (Figure 3E and 3F). These results indicate that, similar to those in astrocytes [16], lysosomes in microglia also accumulate ATP and exhibit ATP exocytosis in response to various stimuli.

To further characterize the lysosomal exocytosis in microglia, we incubated cells with fluorescent FM dyes, which selectively label the vesicles exhibiting functional exocytosis through the endocytosis-exocytosis recycling pathway [25]. We found that AM1-43, a fixable FM1-43 analogue that is largely preserved after immunochemical procedures [16, 26], labeled a population of vesicles that were immunopositive for the lysosomal enzyme cathepsin D and the lysosomal membrane protein LAMP1 (Figure 4A, 4B and 4E), but not for the endosomal marker EAA1 (Figure 4D and 4E). FM2-10, another type of FM dye, also selectively accumulated in lysosomes labeled

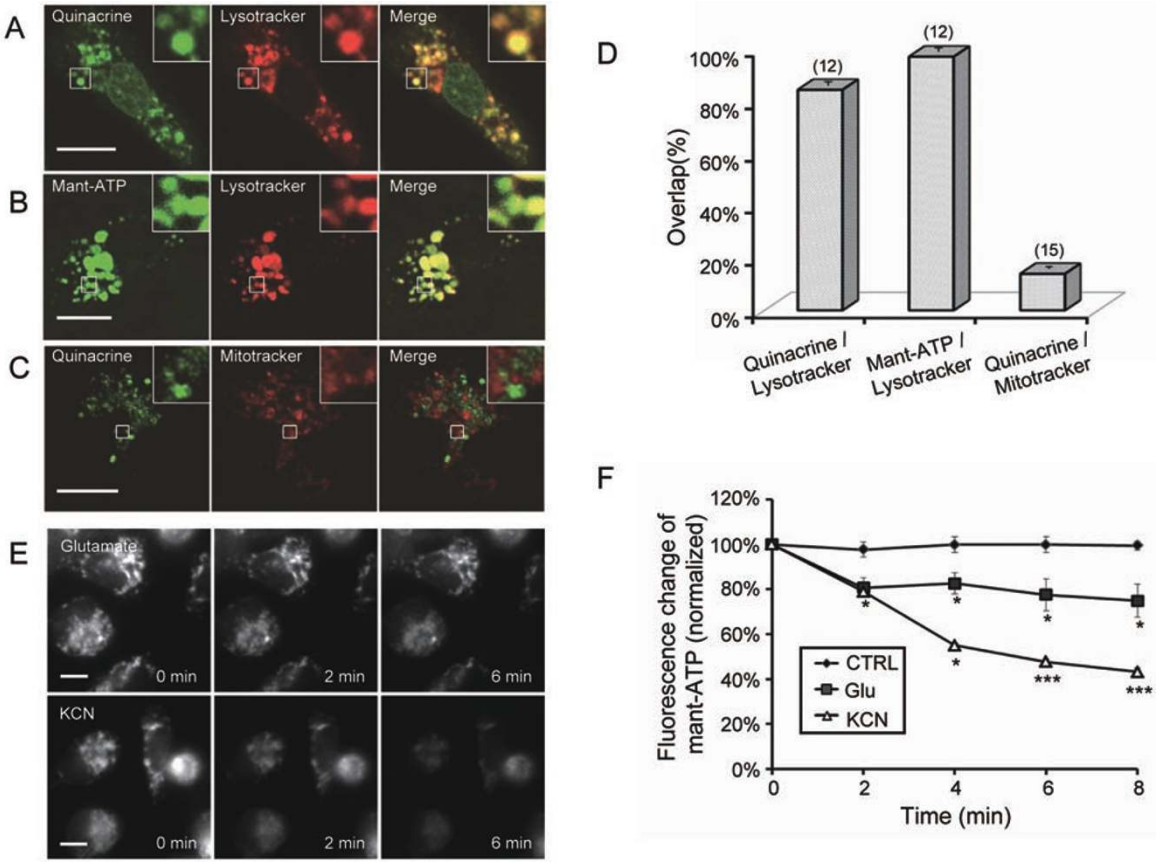

Figure 3 ATP accumulates in and is released from microglial lysosomes. **(A**, **B)** Example images showing selective accumulation of the ATP marker quinacrine (green, **A**) and the nucleotide analogue mant-ATP (green, **B**) in microglial lysosomes labeled with lysotracker (red). Scale bars, 10 μm. **(C)** Example images show that quinacrine (green) weakly accumulated in mitochondrion (mitotracker, red). The boxed areas in **(A**-**C)** are shown at a higher magnification in the insets. **(D)** Summary of the colocalization ratio of quinacrine or mant-ATP with lysotracker or mitotracker as shown in **A**-**C**. The number associated with each column refers to the number of cells examined. **(E)** Time-lapse images of intensity changes of the mant-ATP fluorescence signal in microglia before (0 min), 2 min and 6 min after treatment with glutamate (top panels, Glu, 1 mM) or KCN (bottom panels, 2 mM). Scale bars, 10 μm. **(F)** Averaged intensity changes of the mant-ATP fluorescence signal induced by Glu or KCN as shown in **E**. CTRL, control group without any treatment. Data are normalized to the average fluorescence intensity measured before Glu or KCN treatment. $^{*}P < 0.05$, $^{**}P < 0.01$ and $^{***}P < 0.001$ compared with averaged data obtained before application of Glu or KCN.

with LysoTracker Green DND-26 (LysoTG, Figure 4C and 4E).

We found that the density of membrane surface immunostaining with LAMP1, an indication of fusion of the lysosomal membrane with the plasma membrane [12, 16], was significantly increased by treatment with 1 mM ATP (Figure 5A and 5B). Furthermore, perfusion of 1 mM ATP induced significant destaining of the FM2-10-labeled puncta that was blocked when cultures were loaded with the membrane-permeable Ca^{2+} chelator BAPTA-AM (bis-(o-aminophenoxy) ethane-N,N,N′,N′-tetra-acetic acid acetoxymethyl ester) in Ca^{2+}-free solution (Figure 5C) or treated with P2Y receptor antagonist RB-2 (Figure 5D). Thus, ATP induced Ca^{2+}-dependent lysosomal exocytosis in microglia. This notion was further supported by the finding that perfusion of ATP dose-dependently induced transient intracellular Ca^{2+} elevation in cultured microglia (Figure 6A and 6B), a response that was significantly suppressed in the presence of 2 μM RB-2 (Figure 6C). Furthermore, we found that pulse application of ATP through micropipette (1 mM ATP in pipette), which created ATP concentration gradient to induce microglial migration (Figures 1 and 2), also evoked repetitive Ca^{2+} transients in surrounding microglia (Figure 6D and 6E).

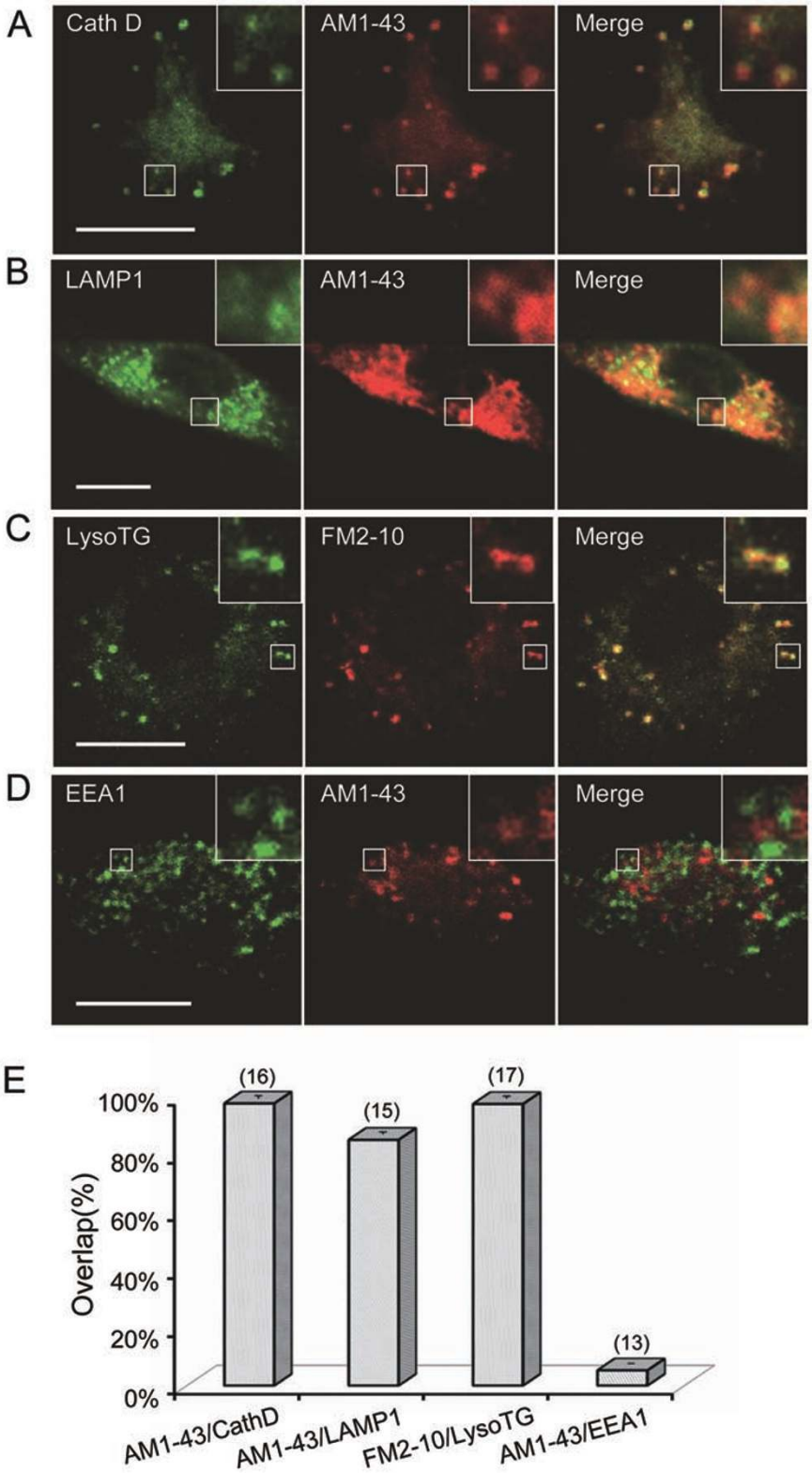

Figure 4 Incubation of microglia with FM dyes selectively labels lysosomes. Confocal images of cultured microglia labeled with lysotracker **(C)** or immunostained with cathepsin D **(A)**, LAMP1 **(B)**, or EAA1 **(D)**, after loading with AM1-43 (red, **A**, **B**, and **D**) or FM2-10 (red, **C**). Right panels: overlay of the two fluorescence signals. The boxed areas in **A**-**D** are shown at a higher magnification in the insets. Scale bars, 10 μm. **(E)** Summary of the colocalization ratio of AM/FM dyes with various markers as shown in **A**-**D**. The number above each column refers to the number of cells examined for each condition.

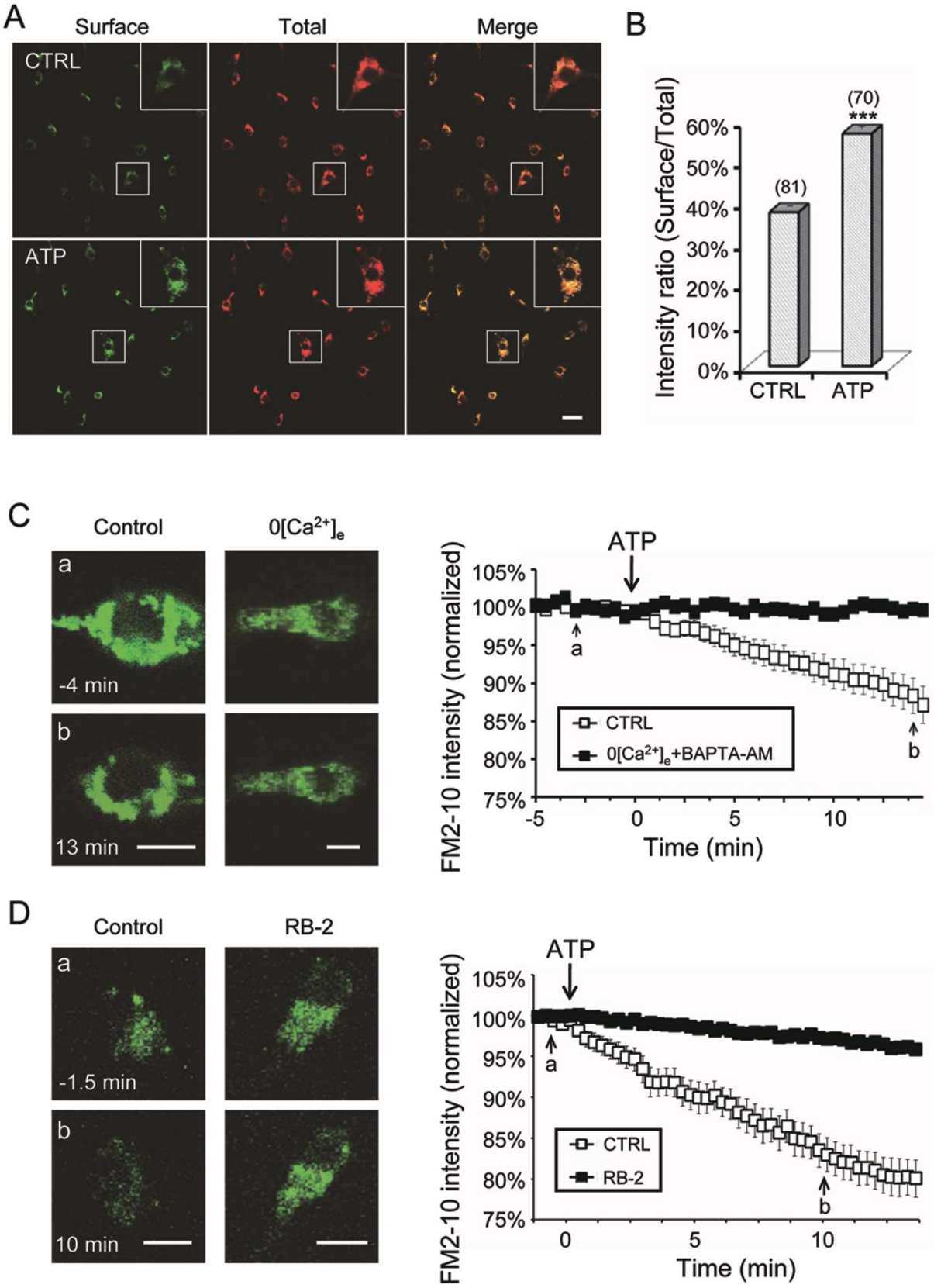
A
Surface
Total
Merge
CTRL
ATP
B
Intensity ratio (Surface/Total)
60%
50%
40%
30%
20%
10%
0%
(81)
(70)
***
CTRL
ATP
C
Control
0[Ca2+]e
a
-4 min
b
13 min
ATP
FM2-10 intensity (normalized)
105%
100%
95%
90%
85%
80%
75%
CTRL
0[Ca2+]e+BAPTA-AM
-5
0
5
10
Time (min)
D
Control
RB-2
a
-1.5 min
b
10 min
ATP
FM2-10 intensity (normalized)
CTRL
RB-2
0
5
10
Time (min)

Involvement of lysosomal exocytosis in microglial migration

To directly determine whether lysosomes are involved in microglial chemotaxis, we incubated cultures with glycylphenylalanine-2-naphthylamide (GPN), a substrate of the lysosomal exopeptidase cathepsin C that selectively induces lysosome osmodialysis [16, 27]. We found that the cell mobility (data not shown) and ATPγS-induced migration (Figure 7A) were reversibly blocked in microglia treated with 100 μM GPN, suggesting a crucial role of lysosomes in microglial migration.

The small GTPase Rab27a plays a critical role in controlling the trafficking and exocytosis of secretory lysosomes or lysosome-related organelles as well as in exosome secretion [28], including melanosomes in melanocytes, dense granules in platelets, insulin granules in pancreatic β-cells, lytic granules in cytotoxic T lymphocytes, and MHC class II compartments in antigen-presenting cells including macrophages and dendritic cells [9, 10]. We thus further determined whether Rab27a affects microglial migration using the Rab27a mutant mouse (ashen), a model for human Hermansky-Pudlak syndrome characterized by hypopigmentation, prolonged bleeding time and platelet storage pool deficiency [29]. We found that although the 1 mM ATPγS-induced migration rate of microglia cultured from ashen mice was not significantly different from that cultured from wild-type mice (Figure 7B), 0.5 mM or 0.1 mM ATPγS-induced migration of microglia, especially those located 120 μm or further from the pipette tip, was significantly inhibited in ashen mice (Figure 7C and 7D, Supplementary information, Movies S5 and S6). There was no significant difference in cell mobility between untreated wild-type (1.96 ± 0.05 μm/min, n = 61 cells) and ashen (1.95 ± 0.06 μm/min, n = 59 cells) microglia.

Discussion

ATP is an important signaling molecule that mediates cell-cell interactions in the brain [3-8, 16, 20, 30]. In response to laser-induced brain injury, microglia rapidly extend processes towards the injury site without apparent cell body migration, a response that is mediated by ATP [3, 5]. Since the signal inducing microglial process extension remains functional for more than 30 min, it was suggested that ATP release from injured neural cells may only initiate the early-phase response, whereas a regenerative ATP release in the surrounding neural cells, perhaps astrocytes, may be required to fuel a sustained response [3]. By establishing an *in vitro* migration assay model, we were able to directly observe and quantify the rapid whole cell migration induced by ATP as well as the dynamic changes in microglial processes. The directional extension of processes and migration of the cell body may share the same signaling mechanism. The absence of injury-induced cell body migration in brain tissue within the limited observation period reported previously [3, 5] may be explained by the tight cell adhesion in intact tissue that may prevent rapid movement of the cell body. Our results provide direct evidence that ATP released from microglia themselves is critical for regeneratively creating ATP so that the local signal can be amplified and propagated to induce migration of remote microglia.

It should be pointed out that, in addition to microglia, other types of neural cells, in particular astrocytes, may also contribute to regenerative ATP signaling in the brain [31]. Our previous study showed that lysosomal exocytosis in astrocytes is responsible for the ATP-mediated Ca^{2+}

Figure 5 ATP-induced Ca^{2+}-dependent lysosomal exocytosis in microglia. **(A)** Example images showing expression of lysosome membrane protein LAMP1 on the plasma membrane surface (green) of microglia, as revealed by living immunostaining with anti-LAMP1 that recognizes the luminal domain of LAMP1 before permeabilizing the cells with methanol. The second immunostaining of the cells with anti-LAMP1 after permeabilization reveals the cytoplasmic as well as surface expression of LAMP1 (total, red). The detailed protocol of living surface immunostaining of LAMP1 was described in Materials and Methods. Note significantly increased surface staining in ATP-treated cultures (lower panels). The boxed areas are shown at a higher magnification in the insets. Scale bar, 20 μm. **(B)** Summary data showing the ratio of surface/total anti-LAMP1 staining in control (CTRL) and ATP-treated cultures as shown in **A**. The number above each column refers to the number of cells examined. ***P < 0.001 compared with the control group. **(C)** Left panels, example images of FM2-10-labeled puncta in cultured microglia 4 min before (a) and 13 min after (b) treatment with 1 mM ATP. Scale bar, 10 μm. Right panel, averaged data from time-lapse imaging of the percentage changes of the FM2-10 signal induced by ATP in cultured microglia with or without pre-incubation in solution containing 0 mM Ca^{2+} and 10 μM BAPTA-AM (Ca^{2+} buffer). Data are normalized to the average fluorescence intensity measured before ATP application. Arrows marked (a) and (b) indicate the time points at which images were taken for left panels (a) and (b), respectively. **(D)** Left panels, example images of FM2-10-labeled puncta in cultured microglia 1.5 min before (a) and 10 min after (b) treatment with 1 mM ATP. Scale bar, 10 μm. Right panel, averaged data from time-lapse imaging of the percentage changes of the FM2-10 signal induced by 100 μM ATP in cultured microglia with or without pre-incubation in solution containing 2 μM RB-2. Data are normalized to the average fluorescence intensity measured before ATP application.

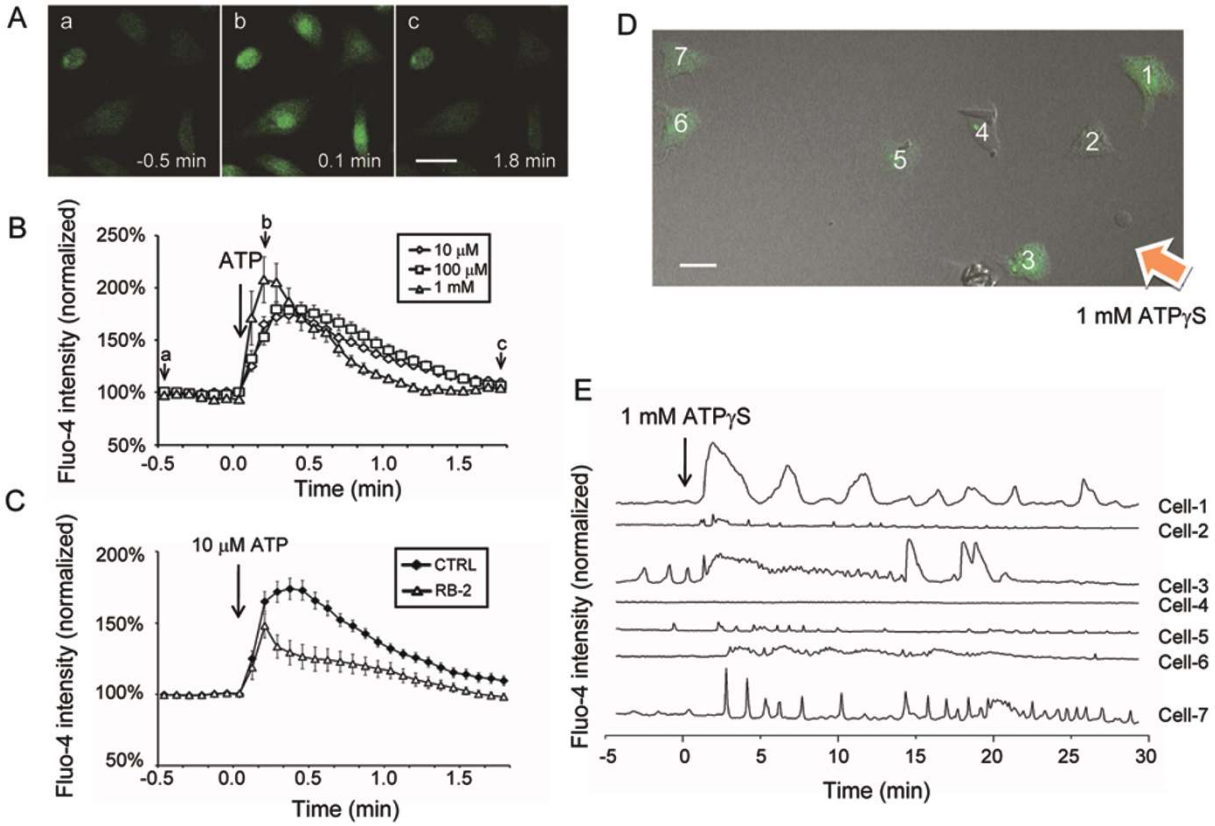

Figure 6 ATP-induced Ca^{2+} signaling in microglia. **(A)** Example fluorescence images of cultured microglia loaded with the Ca^{2+} dye Fluo-4 AM, showing Ca^{2+} signaling before (left panel), during (middle panel), and after (wash, right panel) application of 1 mM ATP. Scale bar, 20 μm. **(B)** Averaged data of the time-lapse imaging of transient fluorescence changes in the Fluo-4 signals in microglia induced by 10 μM (open diamonds), 100 μM (open squares), and 1 mM (open triangles) ATP, respectively. Data are normalized to the average fluorescence intensity measured before ATP application in each cell. **(C)** Averaged data of the time-lapse imaging of Ca^{2+} signal change in the Fluo-4 AM-loaded microglia induced by 10 μM ATP in the absence (filled diamonds) and presence of 2 μM RB-2 (open triangles). Data are normalized to the average fluorescence intensity measured before ATP application in each cell. **(D)** Superimposed fluorescence and phase contrast image of cultured microglia loaded with Fluo-4 AM and exposed to an ATPγS gradient created by pulsatile application of 1 mM ATPγS in the pipette positioned at the lower left corner as indicated by the orange arrow. **(E)** Time course of Fluo-4 fluorescence signals from cells shown in **D**. Traces 1-7 correspond to cells 1-7 labeled in **D**. The arrow marks the time when pulsatile application of ATP started.

wave propagation in cultured astrocytes [16]. The finding that a blocker of connexin channels, which are highly expressed in astrocytes, inhibits the injury-induced directional extension of microglial processes also suggests the involvement of astrocytic signaling in the injury-induced chemotaxis of microglia [3]. However, connexin inhibitors may also have non-specific effects. Whether or not ATP release from astrocytes indeed contributes to the injury-induced chemotaxis of microglia requires further intensive study.

In response to various pathological stimuli, microglia are rapidly activated and secrete a variety of substances including cytokines and neurotrophic factors [1, 32, 33]. However, the mechanism of microglial secretion is largely unknown. Using multiple approaches, we demonstrated here that lysosomes in microglia accumulated abundant ATP and exhibited Ca^{2+}-dependent exocytosis in response to various stimuli. Interestingly, a similar mechanism of ATP secretion has also been demonstrated in astrocytes [16]. Thus, lysosomal exocytosis may be a general mechanism for ATP release in glial cells, in contrast to that in neurons, where ATP is co-released with other neurotransmitters from synaptic vesicles [34].

The idea that ATP-induced ATP release from microglial lysosomes contributes to microglial chemotaxis is further supported by the finding that ATP-induced micro-

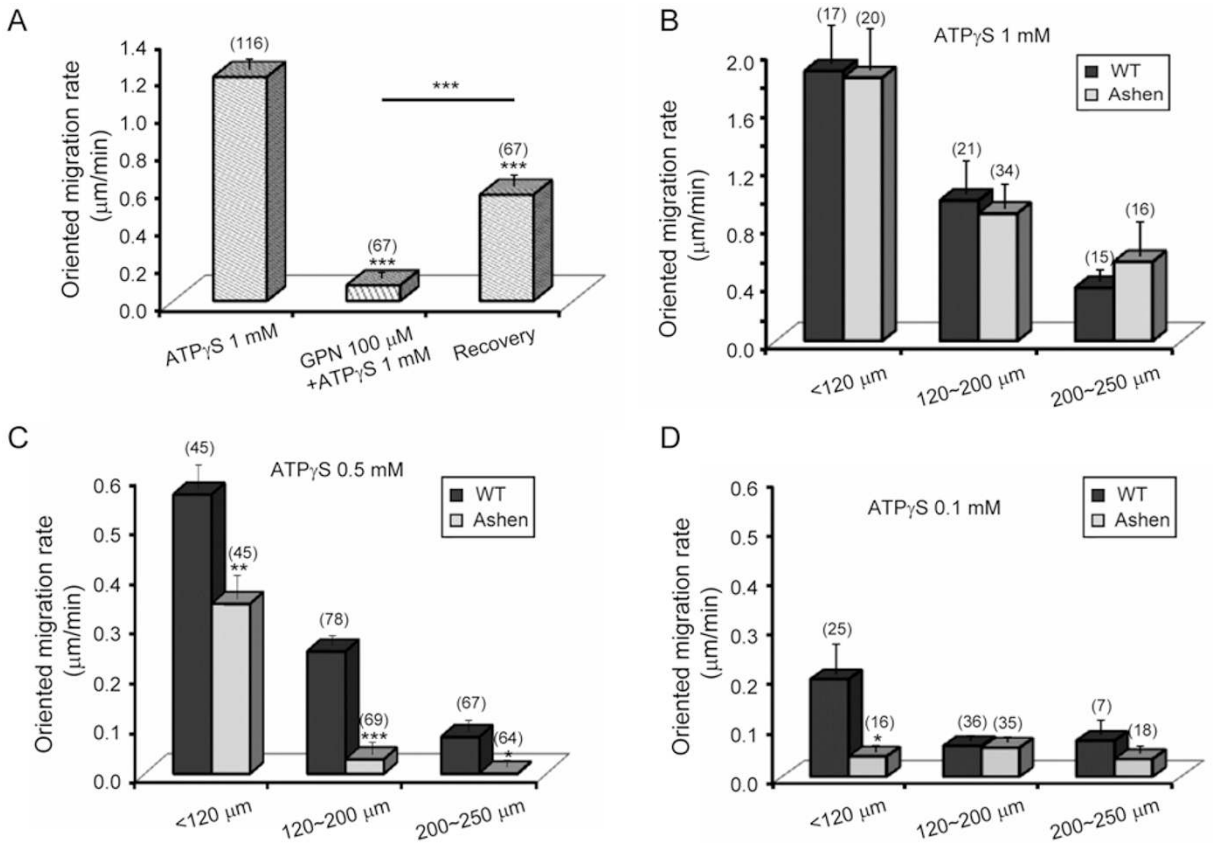

Figure 7 Involvement of lysosomes in ATPγS-induced microglial chemotaxis. **(A)** Averaged data showing the migration rate of cultured microglia induced by puffing 1 mM ATPγS before (ATPγS), during (ATPγS + GPN), and 20 min after washout of 100 μM GPN treatment (recovery). The number above each column refers to the number of cells examined. Note that cells in the whole imaging field, including those 250 μm away from the pipette tip, were included for calculation. ***P < 0.001 compared with control (before GPN treatment) or between the two groups indicated. **(B-D)** Averaged migration rates of microglia from wild-type (WT) and ashen mice, induced by puffing 1 mM **(B)**, 0.5 mM **(C)**, or 0.1 mM **(D)** ATPγS. Note the much more decreased migration rate of remote microglia (> 120 μm from the pipette tip) from ashen mice in **C** and **D**. The number above each column refers to the number of cells examined. **P < 0.01 and ***P < 0.001 compared with the corresponding WT group.

glia migration critically depends on lysosomal function. That is, the cell mobility and directional migration were inhibited in microglia treated with GPN that induced lysosomal osmodialysis. It is unlikely that cell viability was affected by GPN, because the mobility as well as the migration responses largely recovered 20 min after washout of GPN (Figure 7A). Furthermore, the migration induced by 0.5 or 0.1 mM ATPγS was dramatically inhibited in Rab27a-deficient microglia (Figure 7C and 7D), consistent with the important role of Rab27a in the trafficking and exocytosis of lysosomes [9, 10]. The result that the microglial migration induced by 1 mM ATPγS was not significantly affected in Rab27a-deficient mice (Figure 7B) suggest that other subtypes of Rab GTPase, for example Rab27b [28, 35, 36], may partially compensate for the lysosome deficiency in these mice. Rab27a has been suggested to be associated specifically with secretory lysosomes or lysosome-related organelles in some cells derived from the hematopoietic lineage [9, 10], from which microglia are also considered to be derived. It should be pointed out that although our data from Rab27a mutant mice are consistent with all the other evidence that we collected for the involvement of lysosomal exocytosis in microglia chemotaxis, the reduced microglia chemotaxis in Rab27a mutant mice may be also caused by other mechanisms, given the reports that Rab27a is involved in the regulated secretion of secretory granules and exosomes [28]. Nevertheless, our results, together with previous findings that lysosomes in monocytes and microglia are involved in cytokine re-

lease [13-15], suggest that lysosomes in microglia may be classified as secretory lysosomes, which may become potential targets for developing therapeutic treatments of neurodegenerative diseases and brain injury.

Materials and Methods

Reagents

Minimum essential medium (MEM), Leibovitz's L-15 medium (L15), fetal bovine serum (FBS), trypsin and quinacrine were from Invitrogen. Adenosine 5′-triphosphate disodium salt (ATP), adenosine 5′-(3-thiotriphosphate) tetralithium salt (ATPγS), GPN, RB-2, apyrase and glutamate were from Sigma. KCN was from Sinopharm Chemical Reagent Co. AM1-43, FM2-10, LysoTracker Red DND-99, LysoTracker Green DND-26, MitoTracker Red CM-H_2XRos, mant-ATP and Fluo-4 were from Molecular Probes.

Microglial culture

The use and care of animals followed the guidelines of the Shanghai Institutes for Biological Sciences Animal Research Advisory Committee (Shanghai, China). Primary microglial cultures were prepared as reported previously [37] with slight modifications. In brief, cerebral cortex was dissociated from P0-2 Sprague-Dawley rats, devoid of meninges and blood vessels. Tissue was digested by 0.25% trypsin for 15 min at 37 °C. The digestion was stopped by MEM containing 10% (vol/vol) FBS. After mild mechanical trituration, the isolated cells were plated on 75 cm^2 flasks pre-coated with poly-D-lysine (Sigma). The cultures were maintained at 37 °C in a humidified incubator with 5% CO_2/95% air, and the medium was changed every 2 days. After 8-12 days of primary cultivation, microglia were separated from other cell types by slight shaking. The supernatant containing microglia was centrifuged at 1 000× *g* at 4 °C for 5 min. The precipitate was re-suspended and seeded on 8 × 8 mm^2 coverslips (about 2 × 10^4 cells each). After a 30-min attachment period, cells were extensively washed with MEM containing 10% FBS and kept for 1-3 days before experiments. The purity of cultured microglia was > 95%, as assessed by immunostaining with the microglia-specific marker anti-CD 11b.

In some experiments, microglial cultures were prepared from Rab27a mutant mice (C3H/HeSn-*Rab27a^{ash}/J*, ashen mice, Jackson Laboratories). Mutant mice were maintained by breeding homozygous males with heterozygous females. The presence of the ashen Rab27a mutation was confirmed in mutant mice by appropriate reverse transcription polymerase chain reaction (RT-PCR) procedures. Age-matched C3H/HeSn mice were used as background controls.

Chemotaxis assay

Microglial cells from rats or mice on coverslips were placed in a temperature-controlled stage incubator at 33 °C with mineral oil overlaid on the extracellular solution (ECS) to keep the temperature and osmolarity stable. ECS contained 140 mM NaCl, 1 mM KCl, 1 mM $CaCl_2$, 10 mM HEPES, 1 mM $MgCl_2$, 10 mM D-glucose, pH 7.3. Chemotaxis studies were performed using an Olympus microscope (IX50, Japan) connected to a JVC camera (TK-C1381, JVC, Japan). Repetitive pressure injection of picoliter volumes of solutions containing ATP or ATPγS was applied through a micropipette with a tip opening of ~2 μm. The pressure was applied with an electrically-gated pressure application system (Picosprizer II, Parker Co.). A standard pressure pulse of 3 psi in amplitude and 20 ms in duration was applied to the pipette at a frequency of 2 Hz using a pulse generator (Nihon Kohden, Japan).

Cells were exposed to a chemoattractant gradient generated by slowly releasing ATP or ATPγS from the micropipette tip placed at the center of the imaging field. Cell migration toward the pipette tip was tracked by obtaining serial brightfield images every 2 min for up to 30 min. Acquisition was performed using an Olympus microscope with a ×20 air objective (LCACH, 0.4NA), and images were obtained using Fluoview software (Fluoview5.0, Japan). From these images, the migration paths of individual cells were plotted and the total distance traveled toward the point source of ATP (the micropipette tip) was measured by Image-Pro Plus 5.1 software (Media Cybernetics, Canada). From these data, the oriented migration speed for each cell was calculated.

Fluorescent dye loading and imaging

Quinacrine (5 μM), an ATP-binding protein, was incubated with LysoTracker Red DND-99 (50 nM) or MitoTracker Red (100 nM) for 10 min at 37 °C. Images were acquired on a confocal microscope (Olympus FV500 IX71, Japan) with a ×60 water-immersion objective (UPLSAPO60XW, 1.2NA) by sequential scanning of the emission lines with excitation at 488 nm for quinacrine, 543 nm for lysotracker or mitotracker and emission at 505-525 nm for quinacrine, and 560 nm for lysotracker or mitotracker. The fluorescence images were collected every 5 s and analyzed using Fluoview 500 software (Olympus). Mant-ATP (50 μM), a fluorescent ATP analogue, was incubated for 5 h followed by further loading with LysoTracker Red DND-99 (50 nM) for 10 min before washing with ECS. Images were taken by confocal microscope (Zeiss LSM510, Germany) using a 40× 0.8NA water-immersion objective with excitation at 720 nm for mant-ATP, 543 nm for lysotracker and emission at 500-530 nm for mant-ATP, 560 nm for lysotracker. A low laser power (< 0.5%) was used to avoid possible fluorescence bleaching.

For time-lapse imaging of the mant-ATP signal, cells were settled on a live cell imaging system based on a Nikon TE-2000E inverted microscope with a 40× 0.6NA air objective, and including a Hamamatsu infrared CCD. A 1 ms exposure time was selected for each time point to avoid photobleaching. Incubation of cultures with glutamate or KCN at the concentrations used had no cell toxicity as detected by lactate dehydrogenase measurement within 6 min after perfusion (data not shown).

Microglia were loaded with 5 μM FM2-10 or 10 μM AM1-43, a fixable FM1-43 analogue that is largely preserved after immunochemical procedures [16], in the culture medium for 2 h and 5 μM Fluo 4-AM for 30 min at 37 °C. The microglia were then washed for 20 min in ECS before transfer to the chamber for imaging under a confocal microscope (Olympus FV500IX71, Japan) with a 60× water-immersion objective (UPLSAPO60XW, 1.2NA). The time course of the change in fluorescence intensity was obtained at an image interval of 5 s, with emission > 560 nm and excitation 488 nm for FM2-10 and emission > 500 nm and excitation 488 nm for Fluo 4-AM. The pinhole was set to the maximum value to acquire the whole cell fluorescence. A low laser power (< 0.5%) was used to avoid fluorescence bleaching. The decrease in fluorescence intensity due to photobleaching was < 5% over 10 min. Data

analysis was performed with Metamorph software (Universal Imaging Corp., Downington, PA, USA) and Fluoview 500 software (Olympus MicroImaging, Inc.).

AM1-43 loading assay

Microglia cultured on coverslips were loaded overnight with 10 μM AM1-43, then washed slightly once with warm phosphate-buffered saline (PBS), fixed for 5 min with freshly-made 4% (w/v) paraformaldehyde (PFA), washed three times without waiting, and permeabilized for 3 min with methanol. The fixed cultures were blocked with 10% bovine serum albumin (BSA, Roche) in PBS for 1 h at room temperature, and then washed three times without waiting. Incubation with primary antibodies diluted to the appropriate concentration in PBS was done overnight at 4 °C. After washing gently with PBS, the cells were incubated with secondary antibody coupled to Cy-5 (1:1 000, Jackson Immuno Research). After washing three times with PBS, the microglia were analyzed by confocal laser scanning microscopy.

Immunocytochemistry

For immunocytochemical experiments, microglia on coverslips were fixed with 4% (w/v) PFA in PBS for 15 min at room temperature, and permeabilized with 0.2% (w/v) Triton X-100 (or methanol for anti-LAMP1 and anti-cathepsin D) for 10 min at room temperature. The fixed cultures were blocked with 10% BSA (Roche) in PBS for 1 h at room temperature. Then the cells were stained with primary antibodies overnight at 4 °C. Cells were washed gently with PBS followed by incubation with secondary antibodies for 1 h at room temperature, and washed with PBS before imaging. The antibodies used for immunostaining were anti-cathepsin D (Santa Cruz), anti-LAMP1 (Stressgen Biotechnologies) and anti-EEA1 (BD Transduction Laboratories).

To estimate the fraction of LAMP-1 expression on the plasma membrane surface over the total cellular LAMP1 level, cells on coverslips were subjected to two rounds of immunostaining. In the first round, immunostaining that recognizes surface expression of LAMP1, living cells were incubated for 30 min with mouse anti-LAMP1 over the ice-cold water [12, 16]. After rinsing in cold PBS, cells were fixed with 4% PFA and incubated with Alexa Fluor 488 goat anti-mouse secondary antibody. In the second round, immunostaining that recognizes both surface and cytoplasmic LAMP1 (total), cells were permeabilized with methanol and stained with mouse anti-LAMP1 conjugated with Alexa Fluor 546 goat anti-mouse secondary antibody. All primary antibodies were used at a 1:500 dilution and secondary antibodies at 1:1 000.

Real-time imaging ATP release

The assay is based on an enzyme reaction driven by two enzymes: hexokinase and glucose-6-phosphate dehydrogenase (G6PD) [38]. In the presence of ATP and glucose, G6PD converts NADP to NADPH, a fluorescence molecule that can be imaged by fluorescence microscopy. The assay mixture contains 2 U/ml hexokinase, 10 mM D-glucose, 2 U/ml G6PD and 2 mM NADP. All components were diluted in ECS. The microscope experiments were performed using a Nikon TE-2000E inverted microscope equipped with a temperature-controlled stage incubator. Based on the fluorescence properties of NADPH, we used a filter set of a 340-nm band-pass exciter with a band width 15 nm and a 445-nm band-pass emitter. Images were acquired by a CCD camera (Cascade 512B, Roper) through an 100× oil objective (Nikon super flour/1.3) with exposure time 700 ms.

Statistical analysis

Data are presented as mean ± s.e.m. Statistical comparisons were assessed with an analysis of variance or Student's *t*-test. $P < 0.05$ was taken as significant.

Acknowledgments

We thank Dr IC Bruce (Zhejiang University, China) for critical comments on the manuscript and Dr XB Yuan (Institute of Neuroscience, SIBS, CAS, China) for valuable discussion. This work was supported by grants from the Major State Basic Research Program of China (2011CB504400, 2011CBA00400) and the National Natural Science Foundation of China (30730037, 30800321).

References

1 Kreutzberg GW. Microglia: A sensor for pathological events in the CNS. *Trends Neurosci* 1996; **19**:312-318.
2 Koizumi S, Shigemoto-Mogami Y, Nasu-Tada K, *et al.* UDP acting at P2Y(6) receptors is a mediator of microglial phagocytosis. *Nature* 2007; **446**:1091-1095.
3 Davalos D, Grutzendler J, Yang G, *et al.* ATP mediates rapid microglial response to local brain injury *in vivo*. *Nat Neurosci* 2005; **8**:752-758.
4 Honda S, Sasaki Y, Ohsawa K, *et al.* Extracellular ATP or ADP induce chemotaxis of cultured microglia through G(i/o)-coupled P2Y receptors. *J Neurosci* 2001; **21**:1975-1982.
5 Nimmerjahn A, Kirchhoff F, Helmchen F. Resting microglial cells are highly dynamic surveillants of brain parenchyma *in vivo*. *Science* 2005; **308**:1314-1318.
6 Cunha RA, Sebastiao AM, Ribeiro JA. Inhibition by ATP of hippocampal synaptic transmission requires localized extracellular catabolism by ecto-nucleotidases into adenosine and channeling to adenosine A1 receptors. *J Neurosci* 1998; **18**:1987-1995.
7 Zimmermann H, Braun N. Extracellular metabolism of nucleotides in the nervous system. *J Auton Pharmacol* 1996; **16**:397-400.
8 Zhang JM, Wang HK, Ye CQ, *et al.* ATP released by Astrocytes mediates glutamatergic activity-dependent heterosynaptic suppression. *Neuron* 2003; **40**:971-982.
9 Blott EJ, Griffiths GM. Secretory lysosomes. *Nat Rev Mol Cell Biol* 2002; **3**:122-131.
10 Griffiths GM. Secretory lysosomes - a special mechanism of regulated secretion in haemopoietic cells. *Trends Cell Biol* 1996; **6**:329-332.
11 Jaiswal JK, Andrews NW, Simon SM. Membrane proximal lysosomes are the major vesicles responsible for calcium-dependent exocytosis in nonsecretory cells. *J Cell Biol* 2002; **159**:625-635.
12 Reddy A, Caler EV, Andrews NW. Plasma membrane repair is mediated by Ca^{2+}-regulated exocytosis of lysosomes. *Cell* 2001; **106**:157-169.
13 Andrei C, Margiocco P, Poggi A, Lotti LV, Torrisi MR, Rubartelli A. Phospholipases C and A2 control lysosome-mediated

IL-1 beta secretion: Implications for inflammatory processes. *Proc Natl Acad Sci USA* 2004; **101**:9745-9750.
14 Duan S, Neary JT. P2X(7) receptors: properties and relevance to CNS function. *Glia* 2006; **54**:738-746.
15 Eder C. Mechanisms of interleukin-1beta release. *Immunobiology* 2009; **214**:543-553.
16 Zhang Z, Chen G, Zhou W, *et al.* Regulated ATP release from astrocytes through lysosome exocytosis. *Nat Cell Biol* 2007; **9**:945-953.
17 Li DD, Ropert N, Koulakoff A, Giaume C, Oheim M. Lysosomes are the major vesicular compartment undergoing Ca^{2+}-regulated exocytosis from cortical astrocytes. *J Neurosci* 2008; **28**:7648-7658.
18 Jaiswal JK, Fix M, Takano T, Nedergaard M, Simon SM. Resolving vesicle fusion from lysis to monitor calcium-triggered lysosomal exocytosis in astrocytes. *Proc Natl Acad Sci USA* 2007; **104**:14151-14156.
19 Lohof AM, Quillan M, Dan Y, Poo MM. Asymmetric modulation of cytosolic camp activity induces growth cone turning. *J Neurosci* 1992; **12**:1253-1261.
20 Haynes SE, Hollopeter G, Yang G, *et al.* The P2Y(12) receptor regulates microglial activation by extracellular nucleotides. *Nat Neurosci* 2006; **9**:1512-1519.
21 Coco S, Calegari F, Pravettoni E, *et al.* Storage and release of ATP from Astrocytes in culture. *J Biol Chem* 2003; **278**:1354-1362.
22 Mitchell CH, Carre DA, McGlinn AM, Stone RA, Civan MM. A release mechanism for stored ATP in ocular ciliary epithelial cells. *Proc Natl Acad Sci USA* 1998; **95**:7174-7178.
23 Sorensen CE, Novak I. Visualization of ATP release in pancreatic acini in response to cholinergic stimulus - Use of fluorescent probes and confocal microscopy. *J Biol Chem* 2001; **276**:32925-32932.
24 Dubinsky JM, Rothman SM. Intracellular calcium concentrations during chemical hypoxia and excitotoxic neuronal injury. *J Neurosci* 1991; **11**:2545-2551.
25 Cochilla AJ, Angleson JK, Betz WJ. Monitoring secretory membrane with FM1-43 fluorescence. *Annu Rev Neurosci* 1999; **22**:1-10.
26 Renger JJ, Egles C, Liu GS. A developmental switch in neurotransmitter flux enhances synaptic efficacy by affecting AMPA receptor activation. *Neuron* 2001; **29**:469-484.
27 Jadot M, Colmant C, Wattiauxdeconinck S, Wattiaux R. Intralysosomal hydrolysis of glycyl-L-phenylalanine 2-naphthylamide. *Biochem J* 1984; **219**:965-970.
28 Ostrowski M, Carmo NB, Krumeich S, *et al.* Rab27a and Rab27b control different steps of the exosome secretion pathway. *Nat Cell Biol* 2010; **12**:19-30.
29 Wilson SM, Yip R, Swing DA, *et al.* A mutation in Rab27a causes the vesicle transport defects observed in ashen mice. *Proc Natl Acad Sci USA* 2000; **97**:7933-7938.
30 Liu GD, Ding JQ, Xiao Q, Chen SD. P2Y6 receptor and immunoinflammation. *Neurosci Bull* 2009; **25**:161-164.
31 Anderson CM, Bergher JP, Swanson RA. ATP-induced ATP release from astrocytes. *J Neurochem* 2004; **88**:246-256.
32 Raivich G. Like cops on the beat: the active role of resting microglia. *Trends Neurosci* 2005; **28**:571-573.
33 Feng Y, Li L, Sun XH. Monocytes and Alzheimer's disease. *Neurosci Bull* 2011; **27**:115-122.
34 Sperlagh B, Vizi ES. Neuronal synthesis, storage and release of ATP. *Semin Neurosci* 1996; **8**:175-186.
35 Tolmachova T, Abrink M, Futter CE, Authi KS, Seabra MC. Rab27b regulates number and secretion of platelet dense granules. *Proc Natl Acad Sci USA* 2007; **104**:5872-5877.
36 Mizuno K, Tolmachova T, Ushakov DS, *et al.* Rab27b regulates mast cell granule dynamics and secretion. *Traffic* 2007; **8**:883-892.
37 Nakajima K, Shimojo M, Hamanoue M, Ishiura S, Sugita H, Kohsaka S. Identification of elastase as a secretory protease from cultured rat microglia. *J Neurochem* 1992; **58**:1401-1408.
38 Corriden R, Insel P, Junger W. A novel method using fluorescence microscopy for real-time assessment of ATP release from individual cells. *Am J Physiol Cell Physiol* 2007; **293**:C1420-C1425.

(**Supplementary information** is linked to the online version of the paper on the *Cell Research* website.)